Zeitschrift für Kristallographie 212, 327–333

Letter

Surface X-ray diffraction on clean and Cs-covered Ag(001)

H. L. Meyerheim*, S. Pflanz

Universität München, Institut für Kristallographie & Angewandte Mineralogie, Theresienstraße 41, D-80333 München, Germany

R. Schuster and I. K. Robinson

University of Illinois, Department of Physics, Urbana IL 61801, USA

Received December 16, 1996; accepted February 10, 1997

Abstract. We have studied the structure of the clean and Cs covered Ag(001) surface, using surface X-ray diffraction. For the clean unreconstructed Ag(001) surface the analysis of the integer-order crystal truncation rods gives evidence for a compression of the first interlayer spacing relative to the bulk by $\Delta d_{12}/d_{\text{bulk}} = -0.8(8)\%$, whereas for the second interlayer spacing we obtain an expansion of $\Delta d_{23}/d_{\text{bulk}} = 1.0(8)\%$. For the first two Ag layers we observe enhanced thermal disorder as expressed by the isotropic mean-squared displacement amplitude, $U = 0.011(1)$ Å^2 at 340 K relative to the bulk value of 0.009 Å^2 at this temperature. Our X-ray results for Ag(001) are in good agreement with previous experimental and theoretical results. The adsorption of 0.25 ML (1 ML = 1.25×10^{15} adatoms/cm^2) Cs on the Ag(001) surface at 170 K leads to the formation of a $c(2 \times 4)$ superstructure. The Cs atoms are found to occupy fourfold hollow sites at $d_{\text{Cs}} = 2.49(20)$ Å above the Ag(001) surface thereby shifting the underlying Ag atoms laterally by 0.029(5) Å from their bulk positions. From the adsorption height we derive an effective Cs radius of 1.78(16) Å. Large anisotropic disorder is observed for the Cs adatoms. Within the harmonic approximation we derive mean-squared displacement amplitudes of $U_{11} = 0.08(1)$ Å^2, $U_{22} = 0.10(1)$ Å^2 and $U_{33} = 0.27(3)$ Å^2. An alternative model, suggested by the very large value of U_{33}, was also tried, in which there are 15% of Ag vacancies in the top layer and a lower Cs site. This 'unusual' model is discussed in the context of current theories of alkali metal induced reconstructions.

* Correspondence author
(e-mail: uk40104@sunmail.lrz-muenchen.de)

I. Introduction

The structure analysis of clean and adsorbate-covered crystal surfaces is an important branch in surface science [1]. Scattering techniques like low energy electron diffraction (LEED) and surface X-ray diffraction (SXRD) are frequently used to determine the positions of adsorbate atoms on single crystal surfaces [2, 3]. In addition, the analysis of clean surfaces is of interest. For metal surfaces many LEED studies have been performed to analyse the relaxations of the normal interlayer spacing between layer (i) and ($i + 1$) relative to the bulk spacing ($\Delta d_{i,i+1}/d_{\text{bulk}}$). In general, compression and expansion of the first and second interlayer spacing are observed. When going deeper into the crystal, these displacements are rapidly damped and are often oscillatory [4]. The general trend for the relaxation of d_{12} is that the lower the surface atomic packing density, the larger the inward contraction [5]. Consequently, the densely packed *fcc*(001) and (111) surfaces exhibit the smallest relaxations with a contraction of about 1%. For the Ag(001) surface the most recent LEED analysis did not find a multilayer relaxation within the error bars of 1.5% [6]. On the other hand for the more open *fcc*(110) surface much larger relaxations have been observed. For example, in a SXRD study of the Cu(110) surface, Helgesen et al. [7] determined a first layer contraction of 7%.

The adsorption of alkali metals (AM) is also of general interest in surface science since these adsorbate systems serve as models for the study of adsorbate induced modification of surface properties [8–11]. Prominent research topics are the alkali-induced lowering of the substrate work function, the metallization of semiconductor surfaces, or their catalytic properties. Structural investigations have revealed quite a number of 'unusual' results such as the AM adsorption at on-top sites as well as the formation of substitutional geometries even on low index surfaces, where simple hollow site adsorption might be expected intuitively [11–19]. Further, AM induced reconstructions

are well known where missing row structures have been determined in a number of studies [20–25]. In all cases it is observed that adsorbate induced reconstructions as well as the formation of substitutional geometries only take place either for AM adsorption at room temperature (RT) or after annealing to RT, whereas for adsorption at low temperatures (≈90 K–150 K) no substantial atomic rearrangement of the substrate structure is observed.

On the basis of these experimental results we used SXRD to analyse the structure of the clean and the Cs-covered Ag(001) surface. For Cs adsorption on Ag(001) at $T = 80$ K different phases have been reported depending on coverage [26], in the present Letter we only concentrate on the $c(2 \times 4)$ superstructure which is related to a Cs coverage of 0.25 monolayer (ML). One ML is defined as 1.25×10^{15} adatoms/cm^2, corresponding to an adlayer density of one Cs per substrate Ag atom.

II. Results and discussion

The measurements were performed at the beamline X16A of the National Synchrotron Light Source (NSLS) in Brookhaven (New York, USA) using the UHV diffractometer operated in the five circle mode as described by Fuoss et al. [27]. Sample cleaning was achieved by repeated Ar^+ ion sputtering (500 eV) followed by annealing at 800 K. A bright (1×1) LEED pattern could be observed after this procedure indicating a well ordered unreconstructed (001) surface. The SXRD measurements on the clean Ag(001) surface were performed at a temperature of 340 K using an X-ray wavelength of 1.09 Å. We monitored in total 108 reflections at grazing X-ray incidence by rotating the crystal around the surface normal [2]. By symmetry equivalence 27 independent reflections are included into the refinement, i.e. we measured the equivalent reflections along all four symmetry equivalent rods. Systematic errors are estimated by the reproducibility of symmetry equivalent reflections which were in the range of about 5% based on $|F|$. It should be noted that for SXRD this is a comparatively accurate data set which in the present case is a prerequisite for obtaining meaningful results although the shape of the individual rods is fairly well reproducible. The averaging over four equivalent reflections provides a good estimate of the systematic error and – importantly – leads to the reduction of the statistical error (see e.g. Ref. [2]). Fig. 1 shows as solid squares the structure factor intensities $|F|^2$ along the (10L) and (11L) crystal truncation rods (CTRs) after correcting the intensity data for active sample area, polarization and Lorentz factor. We use a sample setting corresponding to a body centered bulk unit cell. In this setting the a-, b- and c-axis of the surface unit cell is parallel to $[1\bar{1}0]$, [110] and [001] of the bulk *fcc* unit cell, respectively as shown in Figure 2. A maximum normal momentum transfer of $\Delta q_z = 2.2$ reciprocal lattice units (rlu) could be achieved corresponding to 3.39 Å^{-1} (including the factor 2π).

The CTRs arise due to the truncation of the (semi-infinite) crystal as is discussed in detail in refs. [2, 28, 29]. Due to the lack of periodicity perpendicular to the surface the third reflection index, l, becomes a continuous parameter. Neglecting absorption, the total diffracted intensity along a CTR of a *fcc*(001) surface can be expressed as:

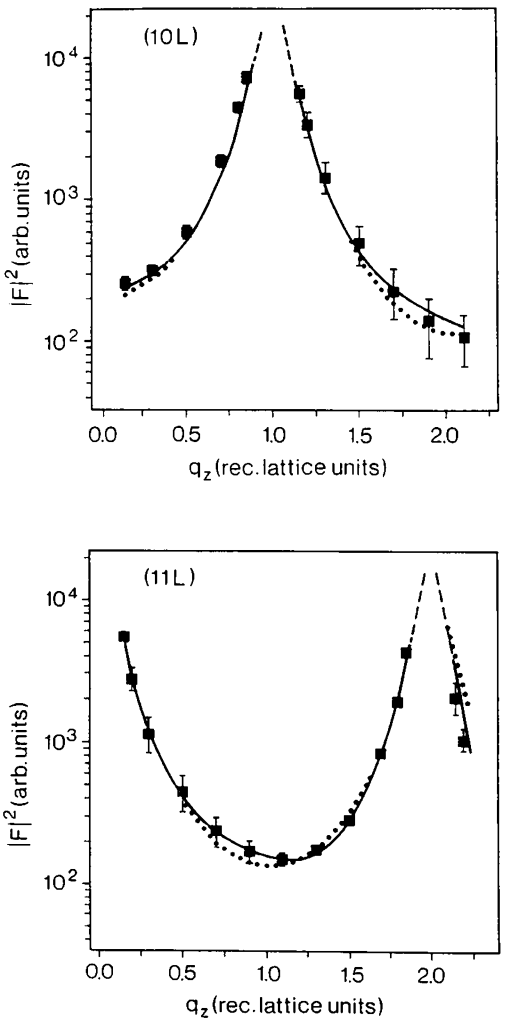

Fig. 1. Measured (solid squares) and calculated structure factor intensities obtained for the clean Ag(001) surface. The best fits including surface relaxations, enhanced surface vibrations and roughness are represented by the solid lines, the intensity distribution calculated for the bulk truncated Ag(001) surface is given by the dotted lines.

$$|F(hkl)|^2 = \left| \frac{f_{Ag} \cdot e^{-M}}{1 - e^{-i\pi(h+k+l)}} + \sum_i f_{Ag} \cdot e^{i2\pi(hx_i + ky_i + lz_i)} \cdot e^{-M_i} \right|^2 \quad (1)$$

where the first term on the right side corresponds to the scattering amplitude of the bulk truncated crystal using the crystal setting mentioned above. For the consideration of surface relaxations additional Ag layers can be taken into account which are represented by the second term. Between successive layers in the bulk there is a phase shift of $\pi(h + k + l)$ since the vector between consecutive layers is (0.5, 0.5, 0.5). Normal relaxations at the surface can be included by shifting the additional Ag atoms out of their 'bulk' positions $z = 0.5$, 1.0, 1.5, etc. Extra Debye-Waller factors e^{-M_i} are included to take account for enhanced surface vibrations. In the present analysis we considered only two surface Ag layers since additional layers did not lead to improved fits. In Figure 1 the solid lines represent the best fits to the data. We obtain $\Delta d_{12}/d_{bulk} = -0.8(8)\%$ and $\Delta d_{23}/d_{bulk} = 1.0(8)\%$. Although the error bars are

large, our results are in agreement with previous theoretical predictions on the normal relaxation of metal surfaces. A first principles calculation of the lattice relaxation by Bohnen, Rodach and Ho [30] found $\Delta d_{12}/d_{bulk} = -1.3\%$ and $\Delta d_{23}/d_{bulk} = 1.0\%$. The error bars were estimated to be in the range of 0.5–1%. Larger relaxations $\Delta d_{12}/d_{bulk}$ were derived by Ning et al. [31] (−3.0%) as well as by Foiles et al. [32] (−1.9%) using the embedded atom method. From the experimental side, LEED experiments on Ag(001) by Li et al. [6] did not find any relaxations within a error bar of 1.5%.

We additionally allowed for a surface Debye-Waller factor where we used a common isotropic mean-squared displacement amplitude U for the first and second layer. The result is $U = 0.012(1)$ Å^2 ($B = 0.95$ Å^2, using the definition $B = 8\pi U$) which is 30% enhanced over the bulk value of 0.009 Å^2 at this temperature (bulk Debye temperature $\theta_D = 225$ K) [33, 34]. Our experiments yield somewhat lower amplitudes than those calculated for the Ag(001) surface by Yang et al. [34]. In their molecular dynamics study the authors found for a temperature of 300 K the values $U_\perp = 0.0152$ Å^2, $U_\parallel = 0.0138$ Å^2 for the first layer and $U_\perp = 0.0113$ Å^2, $U_\parallel = 0.0096$ Å^2 for the second layer, where the subscripts ($\perp$) and ($\parallel$) refer to normal and parallel vibrations, respectively. With our data a distinction between different layers and vibration directions is not possible. However, by averaging Yang's results over both layers and directions and correcting for the sample temperature a theoretical value of $U = 0.014$ Å^2 is obtained for 340 K which is in fair agreement with our data ($U = 0.012$ Å^2). We also fitted the surface roughness expressed by the parameter β as described by Robinson et al. [28] assuming a geometric distribution of layer occupancies. In this model the occupancy is 1.0 for layer 0, layer 1 has a fraction of β occupied sites, layer 2 a fraction of β^2 and so on. Increased roughness leads to a steeper decrease of the intensity away from the bulk Bragg reflections [28, 29]. For Ag(001) we obtained $\beta = 0.130(2)$, a value which can be considered as quite low for metal surfaces.

In order to emphasize the significance of our results the dotted lines in Figure 1 represent the CTR intensity calculated for the bulk truncated crystal, i.e. excluding relaxations and enhanced surface vibrations. With the exception of a common scale factor, the roughness $\beta = 0.158(3)$ was the only fit parameter. The difference between the fits for the bulk truncated crystal and the relaxed surface is small, but significant. Surface relaxations make the CTRs asymmetric with respect to the antiphase position in between the bulk Bragg reflections as can be seen by comparison with the solid lines in Fig. 1. The different fit quality is quantitatively expressed by the agreement parameters. For the optimum fit we determine a weighted residual (R_w) of 5.0% and a goodness of fit (GOF) of 1.4, whereas the calculation for the bulk truncated crystal gives $R_w = 6.7\%$ and $GOF = 1.9$ [35]. For the improved fit both, surface relaxation and enhanced thermal vibrations are about equally important.

In summary, our SXRD data give evidence for an oscillatory relaxation of the first two Ag(001) surface layers by about 1%. This as well as the surface enhanced thermal

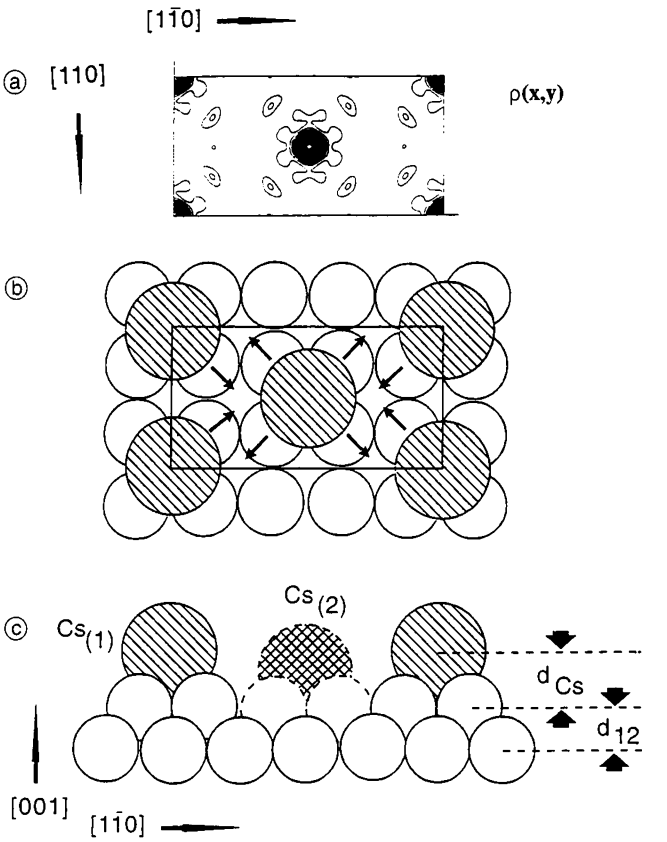

Fig. 2a. Electron density map, $\varrho(x, y)$ of the Cs/Ag(001) $c(2 \times 4)$ superstructure as derived from the in plane fractional order data ($R_w = 5.8\%$, $GOF = 1.04$).

Fig. 2b. Schematic view of the Cs/Ag(001) $c(2 \times 4)$ superstructure projected along the [001] axis. Large and small circles represent Cs and Ag atoms, respectively. The unit cell is indicated by the solid rectangle. The arrows indicate the shifts of the surface layer Ag atoms.

Fig. 2c. Side view of the Cs/Ag(001) $c(2 \times 4)$ superstructure. $Cs_{(1)}$ (hatched) and $Cs_{(2)}$ (crosshatched) indicate the Cs split atoms representing the normal disorder. Top layer Ag defect sites are shown as dashed circles.

disorder is in agreement with theoretical predictions. It also shows that SXRD is capable to determine even small interlayer relaxations.

In a second experiment we studied the Cs/Ag(001) $c(2 \times 4)$ superstructure. Controlled in situ evaporation of Cs at 170 K substrate temperature was achieved using a thoroughly degassed SAES chromate source by simultaneous monitoring a fractional order reflection indicative of the $c(2 \times 4)$ phase. In total 189 superlattice (SL) reflections were measured reducing to 63 independent reflections by symmetry equivalence. In addition 32 CTR reflections along the (10L) and the (11L) rods were measured giving 16 independent reflections after symmetry averaging. Thus, the whole dataset consists of 79 reflections with an average agreement factor of about 6%. As in the case of the measurement of the clean Ag(001) surface, symmetry averaging significantly reduces the error bars of the refined parameters, provided (as is the case here) that there is no substantial disagreement between equivalent reflections as well as between both preparations used for the analysis. It should be noted that the CTR and the SL reflections provide different structural information: The

Table 1. Refined parameters derived for the Cs/Ag(001)-$c(2 \times 4)$ structure. Relative coordinates are given on the basis of the cell dimensions ($a_0 = 5.78$ Å, $b_0 = 11.56$ Å, $c_0 = 4.08$ Å). Parameters denoted by (*) were kept fixed.

Data set	(I) SL	(II) SL + CTR	(III) SL	(IV) SL + CTR
$Cs_{(1)}$				
θ	1.00	1.00	0.85	0.85
$d_{Cs(1)}$ Å	2.49(20)	2.39(20)	2.93(15)	3.00(25)
U_{11} (Å^2)	0.08(1)	0.06(1)	0.08(1)	0.07(1)
U_{22} (Å^2)	0.10(1)	0.09(1)	0.11(1)	0.10(1)
U_{33} (Å^2)	0.27(3)	0.26(3)	0.12(2)	0.16(3)
$Cs_{(2)}$				
θ			0.15	0.15
$d_{Cs(2)}$ Å			1.13	1.13
U_{11} (Å^2)			0.08(1)[a]	0.07(1)[a]
U_{22} (Å^2)			0.11(1)[a]	0.10(1)[a]
U_{33} (Å^2)			0.12(2)[a]	0.16(1)[a]
Ag				
θ	1.00	1.00	0.85	0.85
x	0.2537(6)	0.2524(4)	0.2531(5)	0.2516(3)
y	0.1257(3)	0.1252(2)	0.1259(2)	0.1253(1)
B (Å)^2	0.6*	2.2(4)	0.6*	2.0(3)
β		0.31(3)		0.35(3)
Agreement parameters:				
R_w	9.14%	14.58%	6.18%	11.28%
R_u	13.13%	13.20%	11.38%	13.42%
GOF	1.71	2.83	1.15	2.19
Number of reflections:	63	79	63	79

a: Identical displacement parameters used as for $Cs_{(1)}$. SL and CTR indicate superlattice and crystal truncation rod data sets used, respectively.

CTR reflections are sensitive to both the substrate and the adsorbate structure. In contrast, the SL reflections only probe the superstructure [2].

The Cs atoms adsorb in the fourfold hollow sites of the Ag(001) surface. Fig. 2a shows in a projection along [001] the electron density map of the unit cell which was calculated using the observed SL in-plane structure factors F_{hk0}. Fig. 2b shows the corresponding structural model. The unit cell is indicated by the solid rectangle ($a_0 = 5.78$ Å, $b_0 = 11.56$ Å, plane group $c2mm$). The intense maxima in Fig. 2a are related to the Cs atoms, the weaker ones correspond to top layer Ag atoms which are shifted out of their bulk (1×1)-positions by 0.029(5) Å. Therefore they are observable in the map since only SL reflections were used for the refinement (24 in-plane reflections, $R_w = 5.8\%$, $GOF = 1.04$). In Fig. 2b the Ag-shifts are schematically indicated by the arrows.

The full three dimensional structure refinement includes the analysis of eight SL rods and two CTRs measured up to a maximum momentum transfer of $q_z = 3.00$ Å^{-1} corresponding to 1.95 rlu. The results are listed in Table 1 in columns (I) and (II). These refer to the fits excluding and including the CTR reflections, which both lead to the same results within the error bars. In the following summary of the results we only refer to (I) for simplicity.

The Cs atoms are located 2.49(20) Å above the top Ag-layer corresponding to a nearest Cs–Ag distance of 3.22(16) Å. Within the hard sphere model this can be interpreted by an effective Cs-radius of 1.78(16) Å if a metallic Ag radius of 1.44 Å is assumed. In comparison with previous structure investigations this value is comparatively small. In general effective Cs-radii of about 2.1 Å–2.2 Å are found for high coordination sites [11, 14]. This discrepancy might be attributed to the neglection of the details of the Cs disorder. One example is vibration anharmonicity which can lead to an underestimation of the interatomic distances [25, 36]. In the present case the Cs disorder is very large especially normal to the sample surface, where we find $U_{33} = 0.27(3)$ Å^2. For the in-plane vibrations we obtain $U_{11} = 0.08(1)$ Å^2, $U_{22} = 0.10(1)$ Å^2. Although it is in principle not possible to distinguish between static and dynamic disorder without temperature dependent measurements we may tentatively assume thermal in plane disorder. This assumption is supported by the comparison with temperature-dependent LEED measurements of Löffler et al. [37] on the K/Ni(001) $c(2 \times 4)$ structure which show Debye-like behaviour (Debye temperature $\theta_D \approx 70$ K). At a temperature of 175 K an (isotropic) in plane displacement factor of $U_{ii} = 0.25$ Å^2 ($i = 1, 2$) was derived. Assuming a similar Debye temperature θ_D for the Cs atoms on the Ag(001) surface, the measured in plane displacement amplitudes for K and Cs are reasonably related by their respective atomic masses ($m_{Cs}/m_K = 3.4$) by the factor $U = 3\hbar T/(mk_B\theta_D^2)$, where k_B is the Boltzmann constant. However, for U_{33} our results significantly differ from those of Löffler et al. who obtain $U_{33} = 0.0025$ Å^2 which is much smaller than the in-plane value.

On the basis of the present structure model *GOF*s of 1.71 and 2.83 could be achieved using the datasets (I) and (II), thus indicating that some room is left for improvements. The reason why dataset (II) including the CTRs is worse than (I) where only the SL reflections have been included, might be attributed to a number of additional errors in the CTR data leading to higher systematic errors than estimated. Most importantly, some reflections could be measured only once and at the end of the run where the CTR data were taken, the stability of the adsorbate structure was not verified. This is why we differentiate between both data sets. However, it should be noted, that except from the agreement factors there is no substantial disagreement between the results derived from the different data sets. The consideration of deeper Ag layers did not lead to significantly better agreement.

In order to account for the extremely large value of U_{33} which corresponds to a root mean squared displacement amplitude of $U_{33}^{1/2} = 0.52$ Å, simple thermal disorder does not seem to be reasonable. First we tried anharmonic refinement to account of the Cs disorder. Recent investigations [25] have proven the importance of considering anharmonicity in SXRD analyses. Using the Gram-Charlier formalism up to the fourth order [38] a better agreement with the data was achieved (e.g. using the SL reflections we obtained $R_w = 5.31\%$ and a $GOF = 1.03$). With this model we obtained a bimodal probability density function [38] with two distinct maxima along [001] sepa-

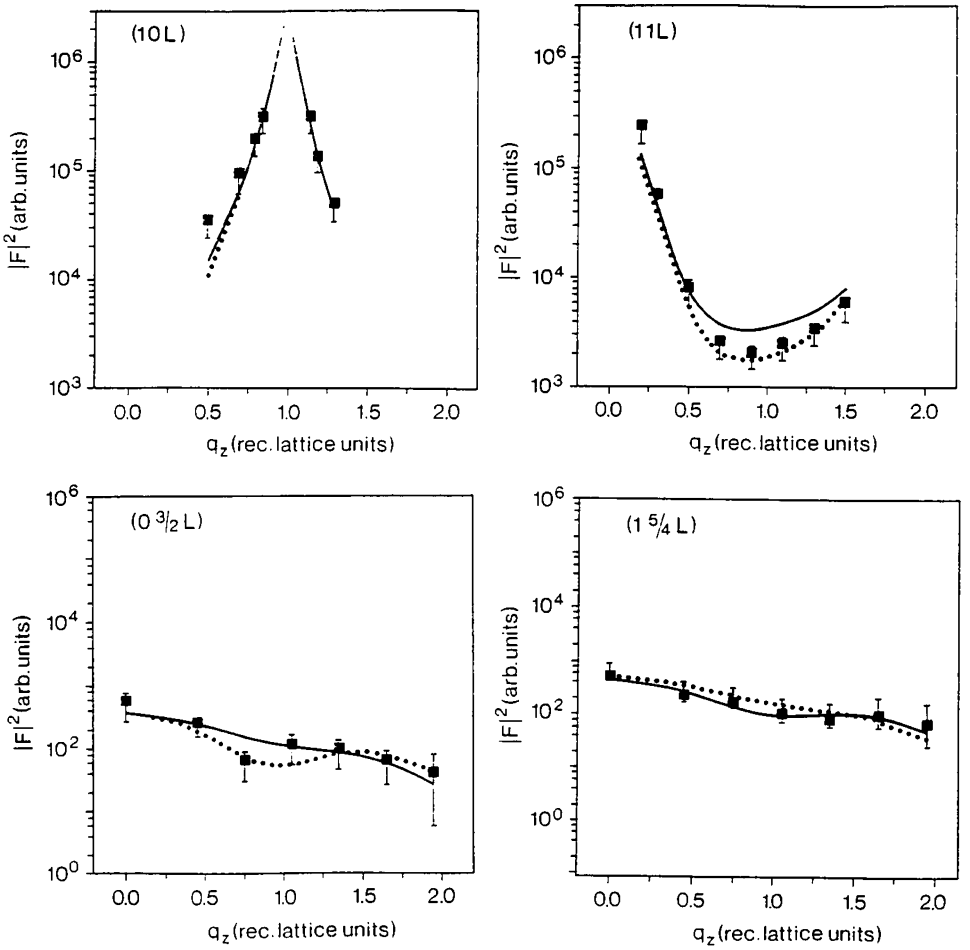

Fig. 3. Measured (solid squares) and calculated structure factor intensities derived for the single Cs adatom model (solid lines) and for the Cs split atom model (dotted lines).

rated by about 1.7 Å. Considering this, a static disorder model seems to be more appropriate. To test this model, calculations using Cs split positions and a partially occupied Ag top layer have been performed. Top layer Ag defects have to be introduced into the model for steric reasons. The results are listed in the columns (III) and (IV) of Table 1. For the best fits occupancies of the Cs split positions of 0.85 for $Cs_{(1)}$ and 0.15 for $Cs_{(2)}$ as well as a partial Ag occupation (0.85) are derived. $Cs_{(1)}$ is located at $d_{Cs(1)} = 2.93$ Å, $Cs_{(2)}$ at $d_{Cs} = 1.13$ Å above the top Ag layer. The adsorption height of 2.93 Å for the more favored position corresponds to an effective Cs-radius of 2.13 Å, a value which is in good agreement with other investigations.

A sideview of this structural model including $Cs_{(1)}$ and $Cs_{(2)}$ is shown in Fig. 2c. Around a $Cs_{(2)}$ atom a cluster of four top layer Ag atoms must be missing, thus the $Cs_{(2)}$ atom resides on top of the second layer of Ag in an on-top site. For $Cs_{(2)}$ we derive a radius of about 1.8(1) Å which is in reasonable agreement with radii (1.9 Å) derived for other on-top structures such as for Cs/Ru(0001) [14]. In this context it should kept in mind that we still observe large normal Cs disorder which is, however now in the same magnitude as the in-plane disorder.

Using this 'split position' model a better agreement with the data can be achieved for both datasets. A very satisfying agreement is obtained using the SL reflections only as expressed by a *GOF* of 1.15 (column III), an improvement relative to the single adatom hollow site model is also observed if we refer to the whole data set including the CTR reflections (IV versus II), although the agreement is less perfect. The difference between the fits related to the structure models is shown in Fig. 3, where we have plotted the calculated intensities for both CTRs and two representative superlattice reflections. The solid and dotted lines correspond to the single Cs adatom and the Cs split atom model, respectively. Especially along the (11L) CTR close to the antiphase condition we obtain a better fit using the split atom model. The CTR data are more sensitive to the surface layer Ag defects than the SL reflections, because the Ag atoms are only slightly shifted out of their bulk (1 × 1) positions and do not contribute strongly to the SL data, whereas the CTR measurements also probe the bulk crystal. Since we realize that this structural model is unusual we tried a number of different models such as the introduction of another Ag-defect site in the second layer leading to a fourfold hollow geometry also for $Cs_{(2)}$. However, all fits assuming more defects or structures different from that shown in Fig. 2(c) yielded *GOF* values which were much worse for those reported here and were therefore discarded.

On the basis of our analysis the Cs/Ag(001) $c(2 \times 4)$ structure – prepared at 170 K in the present investigation – might be classified into the group of 'unusual structures'. It is certainly different from the substitutional AM/Al(111), or AM/Al(100), structure in that it seems to be a frozen intermediate state between a perfect $c(2 \times 4)$ superstructure without any Ag defects and the disordered surface structure without any long range order which is formed by

Cs adsorption at 330 K (data are not discussed in the present Letter). In general, alkali-induced reconstructions are thermally activated and are suppressed at low temperatures (see e.g. ref. [13]), however detailed temperature dependent measurements have not been performed so far. For the Cs/Ag(001) system previous experiments gave some evidence for a temperature dependence of the adsorbate structure. Stolz et al. [26] determined distinct differences in the Cs coverage dependent work function ($\Delta\varphi$) depending on temperature (80 K and 300 K). These were related to a change of the adsorbate/substrate structure. As in our experiments the authors did not find ordered superstructures for Cs adsorption at 300 K. Our CTR data indicate a substantial disruption of the substrate surface upon Cs adsorption. From the theoretical point of view, alkali-induced reconstructions such as the (2×1) phases on *fcc*(110) and (100) surfaces as well as the occupation of substitutional sites for Na and K on Al [12, 13, 18, 19] are generally explained by the energy gain that is achieved if the AM is placed in a higher coordination site and by a more effective screening of the dipole-dipole interaction between the AMs by intervening substrate atoms if the AMs are 'embedded' in the substrate surface [9, 39, 40]. We may speculate that in the present case due to the large Cs atomic size substitutional sites with a replacement of only one substrate atom for one adsorbate atom as observed e.g. for Na/Al(001) $c(2 \times 2)$ might be energetically less favorable since the embedding of the large Cs atom in this way would not lead to an effective screening of the dipole-dipole repulsion. Consequently, a small defect cluster consisting of four missing Ag-atoms is formed allowing the Cs to be embedded more deeply in the surface. Theoretical calculations are required to confirm this picture of Cs induced formation of defect clusters.

Acknowledgments. We (S. P. and H. L. M.) would like to thank AT & T for providing access to the beamline X16A and their hospitality during their visit in Brookhaven. The support of the Bundesministerium für Wissenschaft und Forschung under Grant #05464IAB8 is gratefully acknowledged. Work at the NSLS is supported by the US Department of Energy under DE-AC 012-76CH0016. Additional support came from the University of Illinois Mat. Res. Laboratory under grant DEFG02-96ER45439. The authors also thank R. Wunderlich for the preparation of the figures.

References

[1] Duke, C. B. (Ed.): Surface Science: The first thirty years. Surf. Sci. **299/300** (1994) 1–1054.

[2] Robinson, I. K.: Surface Crystallography. In: *Handbook of Synchrotron*. Vol. 3 (Eds. G. S. Brown; D. E. Moncton), P. 221–266. Amsterdam: Elsevier Publishing 1991.

[3] Van Hove, M. A.; Weinberg, W. H.; Chan, C.-M.: Low energy electron diffraction. Springer Verlag, Berlin, Heidelberg, 1986.

[4] Sokolov, J.; Jona, F.; Marcus, P. M.: Trends in metal surface relaxations. Solid State Commun. **49** (1984) 307–312.

[5] Jona, F.; Marcus, P. M.: Surface structures from LEED. Metal surfaces and metastable phases. In: *The structure of surfaces II*. Springer series in surface sciences, Vol. 11 (Eds. J. F. van der Veen; M. A. van Hove), p. 90–99. Springer Verlag, Berlin, Heidelberg, 1988.

[6] Li, H.; Quinn, J.; Li, Y. S; Tian, D.; Jona, F.; Marcus, P. M.: Multilayer relaxation of clean Ag{001}. Phys. Rev. **B43** (1991) 7305–7307.

[7] Helgesen, G.; Gibbs, D.; Baddorf, A. P.; Zehner, D. M.; Mochrie, S. G. J.: X-ray reflectivity of the Cu(110) surface. Phys. Rev. **B48** (1994) 15320–15325.

[8] Bonzel, H. P.; Bradshaw, A. M.; Ertl, G.: Physics and Chemistry of alkali metal adsorption. Material Science Monographs, Vol. 57. Amsterdam: Elsevier Publishing 1989.

[9] Aruga, T.; Murata, Y.: Alkali metal adsorption on metals. Prog. Surf. Sci. **31** (1990) 61–130.

[10] Stampfl, C.; Scheffler, M.: Theory of alkali metal adsorption on close packed metal surfaces. Surf. Rev. Lett. **2** (1995) 317–343.

[11] Over, H.; Bludau, H.; Gierer, M.; Ertl, G.: Structural properties of alkali metal atoms adsorbed on Ru(0001). Surf. Rev. Lett. **2** (1995) 409–422.

[12] Schmalz, A.; Aminpirooz, S.; Becker, L.; Haase, J.; Nezgebauer, J.; Scheffler, M.; Batchelor, D. R.; Adams, D. L.; Bøgh, E.: Unusual chemisorption geometry of Na on Al(111). Phys. Rev. Lett. **67**(1991) 2163–2166.

[13] Stampfl, C.; Scheffler, M.; Over, H.; Burchhardt, J.; Nielsen, M.; Adams, D. L.; Moritz, W.: Identification of stable and metastable adsorption sites of K adsorbed on Al(111). Phys. Rev. Lett. **69** (1992) 1532–1535.

[14] Over, H.; Bludau, H.; Skottke-Klein, M.; Ertl, G.; Moritz, W.; Campbell, C. T.: Coverage dependence of adsorption site geometry in the Cs/Ru(0001) system: A low energy electron diffraction analysis. Phys. Rev. **B45** (1992) 8638–8649.

[15] Fisher, D.; Chandavarkar, S.; Collins, I. R.; Diehl, R. D.; Kaukasoina, P.; Lindroos, M.: Top site adsorption for potassium on Ni(111). Phys. Rev. Lett. **68** (1992) 2786–2789.

[16] Kerkar, M.; Fisher, D.; Woodruff, D. P.; Jones, R. G.; Diehl, R. D.; Cowie, B.: Structural study of alkali/simple metal adsorption: Rb and Na on Al(111). Phys. Rev. Lett. **68** (1992) 3204–3207.

[17] Adler, D. L.; Collins, I. R.; Liang, X.; Murray, S. J.; Leatherman, G. S.; Tsuei, K.-D.; Chaban, E. E.; Chandavarkar, S.; McGrath, R.; Diehl, R. D.; Citrin, P. H.: Top site adsorption for K on Cu(111) and Ni(111) surfaces. Phys. Rev. **B48** (1993) 17445–17451.

[18] Nielsen, M. M.; Burchhardt, J.; Adams, D. L.; Lundgren, E.; Andersen, J. N.: Anhanced surface vibrations and reconstruction of the Al(111) surface induced by Rb adsorption. Phys. Rev. Lett. **72** (1994) 3370–3373.

[19] Fasel, R.; Aebi, P.; Osterwalder, J.; Schlapbach, L.; Agostino, R. G.; Chiarello, G.: Local structure of $c(2 \times 2)$-Na on Al(001): Experimental evidence for the coexistence intermixing and on-surface adsorption. Phys. Rev. **B50** (1994) 14516–14524.

[20] Hu, Z. P.; Pan, B. C.; Fan, W. C.; Ignatiev, A.: Structure analysis of the Cu(110)-(1×2) surface reconstruction induced by alkali metal adsorption. Phys. Rev. **B41** (1990) 9692–9696.

[21] Schuster, R.; Barth, J. V.; Ertl, G.; Behm, R. J.: Mechanism of the K-induced reconstruction of Cu(110). Surf. Sci. Lett. **247** (1991) L229–L234.

[22] Frenken, J. W. M.; Krans, R. L.; van der Veen, J. F.; Holub-Krappe, E.; Horn, K.: Missing row surface reconstruction of Ag(110) induced by potassium reconstruction. Phys. Rev. Lett. **59** (1987) 2307–2310.

[23] Schuster, R.; Eng, P. J.; Robinson, I. K.: Anomalous coverage behaviour of the Cs–Ag distance on Cs/Ag(110). Surf. Sci. Lett. **326** (1995) L477–L482.

[24] Okada, M.; Tochihara, H.; Murata, Y.: Potassium induced reconstruction of Ag(001). Phys. Rev. **B43** (1991) 1411–1415.

[25] Meyerheim, H. L.; Pflanz, S.; Schuster, R.; Robinson, I. K.: Surface x-ray diffraction on the potassium induced reconstruction of the Ag(001) surface. Physica **B221** (1996) 134–140.

[26] Stolz, H.; Höfer, M.; Wassmuth, H.-W.: TPD, AES, $\Delta\varphi$ and LEED investigations of cesium adsorbed on Ag(001). Surf. Sci. **287/288** (1993) 564–567.

[27] Fuoss, P. H.; Robinson, I. K.: Apparatus for x-ray diffraction in ultra high vacuum Phys. Rev. **222** (1984) 171–176.

[28] Robinson, I. K.: Crystal truncation rods and surface roughness. Phys. Rev. **B33** (1986) 3830–3836.

[29] Meyerheim, H. L.; Robinson, I. K.; Jahns, V.; Eng, P. J.; Moritz, W.: Coverage dependent adsorption sites in the K/Cu(001) system: A crystal truncation rod analysis. Z. Kristallogr. **208** (1993) 73–92.

[30] Bohnen, K. P.; Rodach, Th.; Ho, K. M.: First principles calculation of lattice relaxation at low index surfaces of Ag and Cu. In: *The structure of surfaces III* (Eds. S. Y. Tong; M. A. van Hove), p. 16–23. Springer Verlag, Berlin 1991.

[31] Ning, T.; Yu, Q.; Ye, Y.: Multilayer relaxation at the surface of fcc metals: Cu, Ag, Au, Ni, Pd, Pt, Al. Surf. Sci. **206** (1988) L857–L863.

[32] Foiles, S. M.; Baskes, M. I.; Daw, M. S.: Embedded atom method for the fcc metals Cu, Ag, Au, Ni, Pd, Pt, and their alloys. Phys. Rev. **B33** (1986) 7983–7991.

[33] Morabito, J. M.; Steiger, R. F.; Somorjai, G. A.: Studies of the mean displacement of surface atoms in the (100) and (110) faces of silver single crystals at low temperatures. Phys. Rev. **179** (1969) 638–644.

[34] Yang, L.; Rahmann, T. S.; Daw, M. S.: Surface vibrations of Ag(001) and Cu(001): A molecular dynamics study. Phys. Rev. **B44** (1991) 13725–13733.

[35] The residua are given $R_u = \Sigma_{hkl} ||F_{hkl}^{obs}| - |F_{hkl}^{calc}|| / \Sigma_{hkl} |F_{hkl}^{obs}|$ and $R_w = (\Sigma_{hkl} w_{hkl} ||F_{hkl}^{obs}| - |F_{hkl}^{calc}||^2 / \Sigma_{hkl} w_{hkl} |F_{hkl}^{obs}|^2)^{1/2}$, with $w_{hkl} = \sigma_{hkl}^{-2}$ and $GOF = (N-p)^{-1} \Sigma_{hkl} (||F_{hkl}^{obs}| - |F_{hkl}^{calc}||^2 / \sigma_{hkl}^2)$, where N is the number of reflections and p the number of free parameters.

[36] Meyerheim, H. L.; Robinson, I. K.; Schuster, R.: Temperature-dependent surface X-ray diffraction on K/Ag(001)-(2 × 1). Surf. Sci. **370** (1997) 268–276.

[37] Löffler, U.; Muschiol, U.; Bayer, P.; Heinz, K.; Fritzsche, V.; Pendry, J. B.: Determination of anisotropic vibrations by tensor LEED. Surf. Sci. **331–333** (1995) 1435–1440.

[38] Kuhs, W. F.: Generalized atomic displacements in crystallographic structure analysis. Acta Crystallogr. A**48** (1992) 80–98.

[39] Christensen, O. B.; Jacobsen, K. W.: Theory of alkali metal induced reconstructions of fcc(100) surfaces. Phys. Rev. **B45** (1992) 6893–6898.

[40] Stampfl, C.; Neugebauer, J.; Scheffler, M.: Theoretical evidence for unusual bonding geometry and phase transitions of Na on Al(001). Surf. Rev. Lett. **1** (1994) 213–219.